PROCEEDINGS OF SCIENCE

# Differential photon-jet cross-section measurement with the CMS detector at 7 TeV

**Kadir Ocalan**[∗†]
*On behalf of the CMS Collaboration*
*Necmettin Erbakan University, Buyuk Ihsaniye Mh. Kazim Karabekir Cd. No:82, 42080 Selcuklu, Konya, Turkey*
*E-mail:* kadir.ocalan@cern.ch

The associated production of a photon and one or more jets in pp collisions provides a direct probe into the hard QCD interaction, is sensitive to gluon densities in the proton, and is a major source of background to standard model searches. A measurement of the differential cross section in final states with photon and jet is presented using data collected with the CMS detector at 7 TeV at the LHC. The measured distributions are corrected for efficiency and unfolded for detector effects to be compared with results from event generators. Theoretical predictions are found to be consistent with measured cross-section within total uncertainty.

*Photon 2013,*
*20-24 May 2013*
*Paris, France*

∗Speaker.
†Also at Middle East Technical University, Dumlupinar Bl. No:1, 06800 Cankaya, Ankara, Turkey

 

PoS(Photon 2013)013

## 1. Introduction

Prompt photons are referred to both high-$p_T$ photons from the hard subprocess (direct photons) and from the collinear fragmentation of partons with large $p_T$ (fragmentation photons). Prompt photons do not come from hadron ($\pi^0, \eta, k_s^0, \omega, \rho, ...$) decays. Direct (or pointlike) photon is most probably separated from hadronic environment while fragmentation (or bremsstrahlung) photon is most probably accompanied by hadrons. Compton-like gluon scattering ($qg \rightarrow q\gamma$, dominates at LHC) and quark-antiquark annihilation ($q\bar{q} \rightarrow g\gamma$) are two main leading order mechanisms yielding direct photon in the final states.

Early measurements of prompt photon production were carried out at the ISR (Intersecting Storage Rings) hadron collider at CERN [1]. Later studies established prompt photons as a powerful probe of the dynamics of hard QCD interactions [2]. More recent studies from CMS [3] and ATLAS [4] collaborations presented measurements of isolated prompt photon production cross-section in proton-proton collisisons. More relevantly and recently, photon and associated jet cross-section measurements are published by DØ [5] and ATLAS [6] hadron collider experiments.

Study of final state prompt photon production provides means for testing pQCD calculations ($k_T$ approach, color-dipole, logarithmic resummation techniques, and so on). In particular, compton-like gluon scattering provides direct information on gluon distribution in the proton ([7]-[8] and references therein). Moreover, final state prompt photons appear as a background to Higgs and new physics signatures (H$\rightarrow \gamma\gamma$, graviton, SUSY, and excited fermions). From an experimental point of view, understanding of prompt photon properties are valuable for jet energy calibration, missing energy modeling, and similar measurements in heavy ion collisions.

Compared to existing prompt photon measurements at fixed-target (Fermilab) and collider (ISR, RHIC, SppS, Tevatron) energies, LHC has the capability of probing a couple of orders of magnitude lower kinematical region [9]. Taking advantage of this feature, we present a measurement of triple differential cross-section for photon and associated jet (photon-jet) production from 7 TeV proton-proton collisions with 2.14 fb$^{-1}$ data in the CMS experiment at the LHC [10].

## 2. Analysis

The Compact Muon Solenoid (CMS) is one of two general purpose detectors at the LHC aiming for the Standard Model precision measurements and to search for the Higgs boson and new physics signatures. CMS is composed of several sub-detectors, each with specific purpose. The inner-most part of the detector is the tracker with pixel and strip technologies, followed by the electromagnetic calorimeter (ECAL) and the hadronic calorimeter (HCAL). These three sub-detectors are immersed into solenoid magnetic field of 3.8 T, surrounded by muon chambers at high radius [11].

In this effort, we measure triple differential cross-section of photon in association with jet with respect to $E_T^{\gamma}$, $\eta^{\gamma}$, and $\eta^{jet}$. We require photon transverse momentum ($p_T^{\gamma}$) to be in the band of 40 GeV - 300 GeV in four different photon pseudorapidity ($\eta^{\gamma}$) regions and jet to be both forward and central.

The first item in the analysis flow is photon efficiency measurement. Total efficiency is splitted into photon reconstruction, trigger, identification, and electron rejection (pixel match veto) efficien-

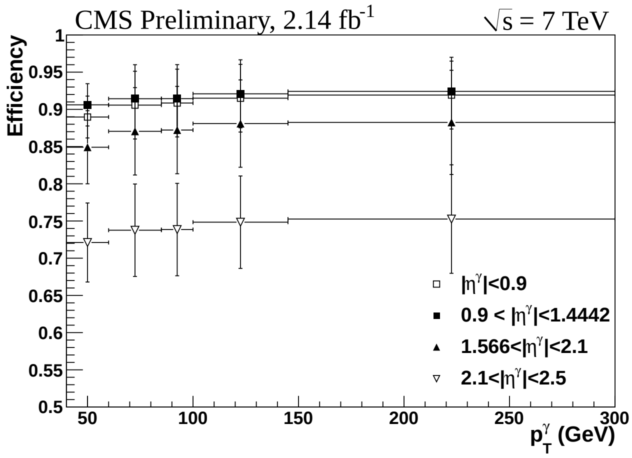


**Figure 1:** Total photon selection efficiency in four different pseudorapidity regions with respect to $p_T^\gamma$. Errors include both statistical and systematical contributions added in quadrature, systematical uncertainties are dominant.

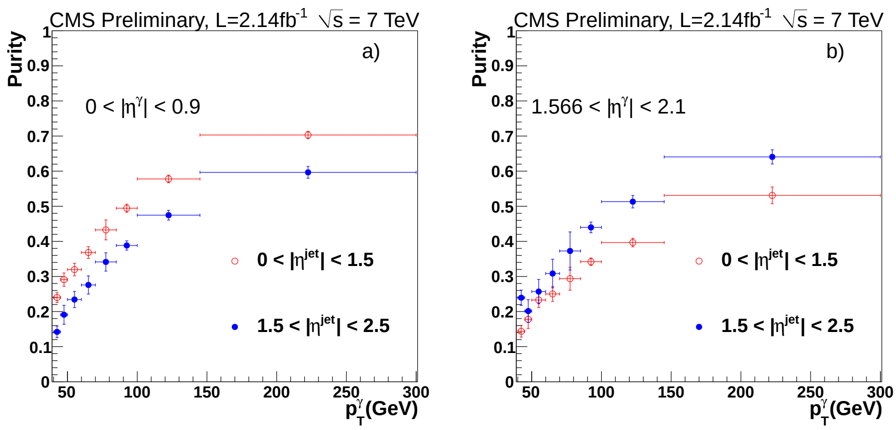


**Figure 2:** Photon purity distributions (left one is for $0 < |\eta^\gamma| < 0.9$, right one is for $1.566 < |\eta^\gamma| < 2.1$) are shown for both central (red points) and forward (blue points) jets.

cies and each item is measured independently. Total efficiency of photon selection is found to be between 72-92 %, lowest in the outer endcap ECAL ($2.1<|\eta^\gamma|<2.5$) as shown in Figure 1.

For prompt photon measurements, jet background ($\pi^0, \eta \to \gamma\gamma$) needs to be suppressed by limiting the energy of other particles surrounding photon in different sub-systems. For this purpose, photon purity measurement is employed in which an isolation variable is used which is the sum of ECAL, HCAL, and Tracker isolations. In this template fitting technique, signal shape is taken from simulation data while background shape is obtained from real collision data. Finally both shapes are fitted to real data to extract photon signal yields by using a utility function which is defined by chi-square function. Example photon purity distributions are given in Figure 2.

Due to detector effects (resolution, calibration, etc.) measured values deviate from true values of photon. For this photon-jet differential cross-section measurement, a mapping between measured and true values has to be evaluated. By using RooUnfold software package [12] and 3D unfolding iterative (Bayesian) approach [13], relationship between masured and true values are taken into account as correction for final cross-section results.

Theoretical predictions for photon-jet processes are obtained both at leading order (LO) using SHERPA [14] and at next to leading order (NLO) using predictions from JETPHOX [15] package. SHERPA can generate hard processes with higher number of outgoing particles in the matrix element. Calculations in SHERPA include higher order tree level matrix elements. The tree level matrix elements of variable photon and QCD parton multiplicity are combined with QCD+QED parton shower. In addition, JETPHOX 1.1 is used and interfaced to LHAPDF version 8.5.4 in order to apply the most recent set of the proton Parton Distribution Functions (PDFs) that is CT10 [16]. Both JETPHOX and SHERPA includes description of fragmentation photons.

Main source of systematic uncertainities comes from efficiency, purity, and unfolding measurements. Differences between shapes from simulated and real data in all sub-measurements added as systematic uncertainty. In addition, parameter of fitting function is shifted and difference is accounted as systematic uncertainty. For theoretical comparision part, changing PDFs and scale factor added theoretical systematic uncertainty to the measurement. In summary, systematic uncertainty is added in quadrature to be 5-15 % for sub-measurements, while theoretical systematical uncertainities are $\sim$4 % for PDFs and $\sim$10 % for scales.

## 3. Results

Events with at least one photon and one jet have been studied with 2.14 fb$^{-1}$ of data in proton-proton collisions at $\sqrt{s} = 7$ TeV. The triple differential cross-section as a function of the transverse momentum of the photon is measured for different orientations between the leading photon and the leading jet as shown in Figure 3.

These different angular orientations are also used to measure eight ratios of the triple-differential cross section ($d^3\sigma/dp_T^\gamma d\eta^\gamma d\eta^{jet}$) providing a measurement of the relative production cross sections for photon-jet system in different pseudorapidity regions and thus for a wide range of parton momentum fraction $x$ as shown in Figure 4.

Although predictions from SHERPA are observed to be lower as compared to JETPHOX, the measured cross section is found to be in good agreement with both LO and NLO generators within total uncertainties. We obtained better data and simulation matches on differential cross-section distribution as compared to previous photon-jet studies from D0̸ [5] and ATLAS [6] experiments.

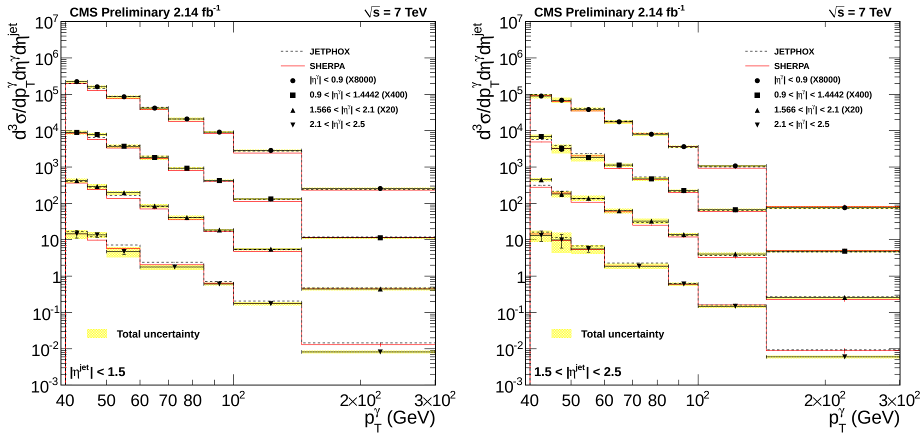


**Figure 3:** Differential cross-section for $0 < |\eta^{jet}| < 1.5$ on the left and for $1.5 < |\eta^{jet}| < 2.5$ on the right. The measured cross sections (markers) in four different ranges of $|\eta^\gamma|$ are compared with the SHERPA tree-level Monte Carlo (solid line) and the NLO perturbative QCD calculation from JETPHOX (dashed line).

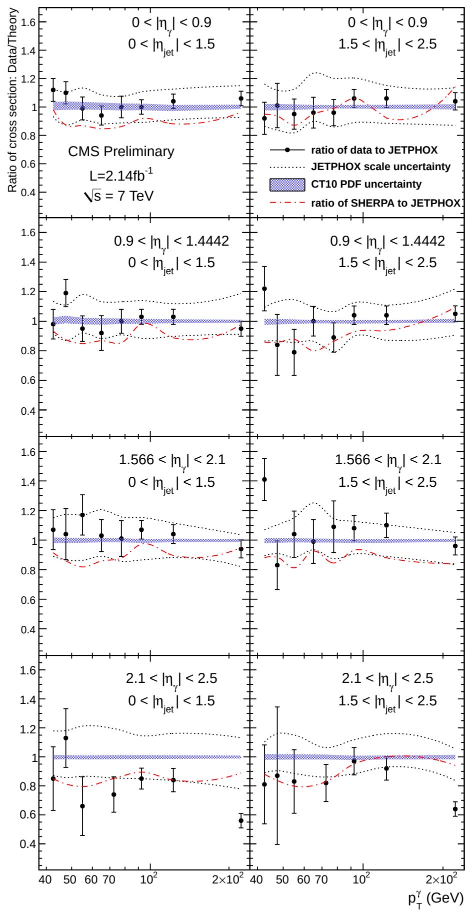


**Figure 4:** The ratios of the measured triple-differential cross section to the NLO QCD prediction using JETPHOX with the CT10 PDF set and scales $\mu_{R,F,f} = 1/2 p_T$. The two dotted lines represent the effect of varying the theoretical scales as described in the text. The shaded region is the CT10 PDF uncertainty. The dash-dotted lines show the ratios of the SHERPA predictions to JETPHOX.

## References

[1] E. Anassontzis et al., *Z. Phys. C* **13** (1982) 277-289, CMOR Collaboration, *Nucl. Phys. B* **327** (1989) 541-568.

[2] UA2 Collaboration, *Phys. Lett. B* **176** (1986) 239-246, UA1 Collaboration, *Phys. Lett. B* **209** (1988) 385-396, UA2 Collaboration, *Phys. Lett. B* **263** (1991) 544-550.

[3] CMS Collaboration, *Phys. Rev. D* **84** (2011) 052011.

[4] ATLAS Collaboration, *Phys. Lett. B* **706** (2011) 150-167, ATLAS Collaboration, *ATLAS-CONF-2013-022*.

[5] DØ Collaboration, *Phys. Lett. B* **666** (2008) 435-445.

[6] ATLAS Collaboration, *Phys. Rev. D* **85** (2012) 092014, ATLAS Collaboration, *ATLAS-CONF-2013-023*.

[7] S. Catani et al., *JHEP* **05** (2002) 028, P. Aurenche et al., *Phys. Rev. D* **73** (2006) 094007.

[8] D. d'Enterria and J. Rojo, *Nucl.Phys. B* **860** (2012) 311-338.

[9] R. Ichou and D. d'Enterria, *Phys. Rev. D* **82** (2010) 014015.

[10] CMS Collaboration, *CMS-PAS-QCD-11-005*, http://cds.cern.ch/record/1525534?ln=en.

[11] CMS Collaboration, *JINST* **3** (2008) S08004.

[12] T. Adye, *Proceedings of the PHYSTAT 2011 Workshop, CERN, Geneva, Switzerland* (2011), CERN-2011-006, pp.313-318, arXiv:1105.1160.

[13] G. D'Agostini, *Nucl. Instr. and Meth. in Phys. Res.* **A362** (1995) 487.

[14] T. Gleisberg et al., *JHEP* **02** (2009) 007.

[15] S. Catani et al., *JHEP* **05** (2002) 028.

[16] H.-L. Lai et al., *Phys. Rev. D* **82** (2010) 074024.